

# Operando Kerr gated Raman spectroscopy of lithium insertion into graphite enables high state of charge diagnostics

Contact [hardwick@liverpool.ac.uk](mailto:hardwick@liverpool.ac.uk)

## A. R. Neale

Stephenson Institute for Renewable Energy, Department of Chemistry, University of Liverpool, Peach Street, Liverpool, L69 7ZF, UK

## D. C. Milan

Stephenson Institute for Renewable Energy, Department of Chemistry, University of Liverpool, Peach Street, Liverpool, L69 7ZF, UK

## F. Braga

Stephenson Institute for Renewable Energy, Department of Chemistry, University of Liverpool, Peach Street, Liverpool, L69 7ZF, UK

## I. V. Sazanovich

Central Laser Facility, Research Complex at Harwell, STFC Rutherford Appleton Laboratory, Harwell Campus, Didcot, Oxfordshire, OX11 0QX, UK

## L. J. Hardwick

Stephenson Institute for Renewable Energy, Department of Chemistry, University of Liverpool, Peach Street, Liverpool, L69 7ZF, UK

## Introduction

To improve the lifetime of lithium ion (Li-ion) cells, methods to reliably probe the cell state of charge to are essential to track lithium inventory loss and understand the relation to key degradation processes in the cell. Nuclear Magnetic Resonance and X-ray/neutron scattering techniques have been demonstrated to probe the full range of intercalation in graphite from  $C_6$  to  $LiC_6$ .<sup>1-3</sup> While Raman spectroscopy has been proven a powerful tool for the analysis of earlier stages of Li intercalation into graphite electrodes, the process is plagued by significant growth in fluorescence/emission signals as the intercalation proceeds between  $Li_{0.5}C_6$  and  $LiC_6$ . Along with a loss of Raman scattering intensity due to increased material conductivities,<sup>4,5</sup> the graphite bands in highly lithiated graphite become swamped by the overlapping fluorescence/emission signals, becoming difficult to reliably observe.

To overcome this challenge, we report here on the first use of *operando* electrochemical Kerr gated Raman spectroscopy to track the changes in the graphitic bands during Li intercalation. We have previously reported on the use of Kerr gated Raman spectroscopy as an effective tool to remove the fluorescence signals of degraded battery electrolyte materials based on the lithium hexafluorophosphate salt and, consequently, reveal the often hidden Raman signals.<sup>6</sup> Herein, a dedicated *operando* measurement cell was designed to facilitate electrochemical measurements under an inert atmosphere and provide laser access to the graphite working electrode *via* an optical viewport. Owing to the efficacy of the Kerr gate in filtering out a significant amount of the problematic emission signals, the graphitic Raman bands could be observed even at very high states of lithiation with much greater clarity than has been achieved by conventional Raman techniques. As such, this creates the opportunity to interrogate high states of charge in graphitic negative electrodes.

## Experimental

**Cell design** - To measure the Kerr gated Raman of electrodes, a modified cell base and sample holder was designed to be coupled with the PEEK body of the ECC-Opto cell by EL-Cell and is shown in Figure 1. Therein, the baseplate was custom built for specific application in the Kerr gated Raman configuration, and a widened window opening (8 mm) was employed to accommodate the 5x5 mm square raster pattern of the excitation laser. A  $CaF_2$  window (0.5 mm) allows the Raman laser to be focused on the graphite electrode for the *operando* measurements.  $CaF_2$  (Crystran) shows only a single Raman peak centred at  $310\text{cm}^{-1}$  and has no fluorescence emission making this compound the best candidate for the cell window. The cell was hermetically sealed inside an Ar glovebox ( $H_2O, O_2 \leq 0.1$  ppm).

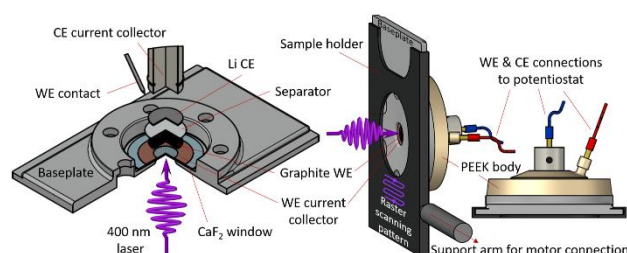


**Figure 1.** A schematic of the *operando* Raman cell assembly. The cell (left), and WE and CE connections, were sealed using PEEK body of the ECC-Opto cell (EL-Cell) and the Kerr gate Raman sample holder system (right) attached to the motor system (not shown) that provides the raster scanning motion during spectra collection.

**Cell preparation** - A free-standing graphite electrode (preparation described previously)<sup>7</sup> based on synthetic microcrystalline graphite (SFG-6, Imerys) was employed as the working electrode in the Li|graphite half-cell. The counter electrode was a polished Li metal disk and the separator (glass fibre, Whatman GF/F) was wetted with a conventional Li-ion battery electrolyte, 1 M  $Li[PF_6]$  in ethylene carbonate/dimethyl carbonate (1:1 by vol). The electrochemical measurements were conducted in parallel with spectroscopic measurements using an SP-150 potentiostat/galvanostat (BioLogic). Kerr gated Raman spectra were collected (below) while the cell was cycled under galvano/potentiostatic control.

**Kerr gated Raman spectroscopy** - The Kerr gated Raman experiments were performed at ULTRA laser facilities (Central Laser Facility, STFC, Rutherford Appleton Laboratories). The Kerr gating system was driven by a ps arm of a Thales deal-beam Ti:Sapphire laser producing 0.8 mJ at 10 kHz repetition rate (pulse duration tuneable between 1 to 3 ps). The optical gating was achieved through inducing Kerr effect in carbon disulphide ( $CS_2$ ) with focussed fundamental beam of the laser. The 2 mm cell with  $CS_2$  was placed between the two crossed polarisers, and the gating 800 nm beam was focussed onto  $CS_2$  into 0.5 mm spot. The polarisation of the gating beam was set at  $45^\circ$  with respect to the polariser. Raman signal of the samples was probed at 400 nm with picosecond laser pulses. Raman probe beam was focused into  $150\ \mu\text{m}$  spot at sample, and the Raman signal was detected at parallel polarisation. Kerr gated Raman spectra were collected under rastering conditions with a laser power of 5 mW; spectra shown is an average of 5 to 10 repeats of 40 s acquisition each.

## Results and discussion

The *operando* Li|graphite half-cell was discharged from open circuit potential (OCP,  $\sim 3$  V vs.  $Li^+/Li$ ) to 0.01 V vs.  $Li^+/Li$  at a C/7 rate (where  $1C = 372\ \text{mA g}^{-1}$  based on the theoretical capacity of graphite) and the Kerr gated Raman spectra were collected continuously during this process. The voltage profile, showing

the typical plateaus associated with structural stages of electrochemical intercalation of  $\text{Li}^+$  into the graphite layers of the electrode,<sup>5</sup> is presented in Figure 2a. The total charge passed exceeds the theoretical capacity for forming  $\text{LiC}_6$  (*i.e.*, where  $x(\text{Li}) = 1$  in  $\text{Li}_x\text{C}_6 = 372 \text{ mAh g}^{-1}$ ), due to established and irreversible decomposition reactions that contribute to formation of solid electrolyte interphase films on graphite electrodes. Additionally, the inset images in Figure 2a show optical images of the working electrode taken before and after Li intercalation. These images, taken *via* the  $\text{CaF}_2$  window, show the associated colour change of the black graphitic electrode at OCP to the gold colour associated with the completely lithiated  $\text{LiC}_6$ .

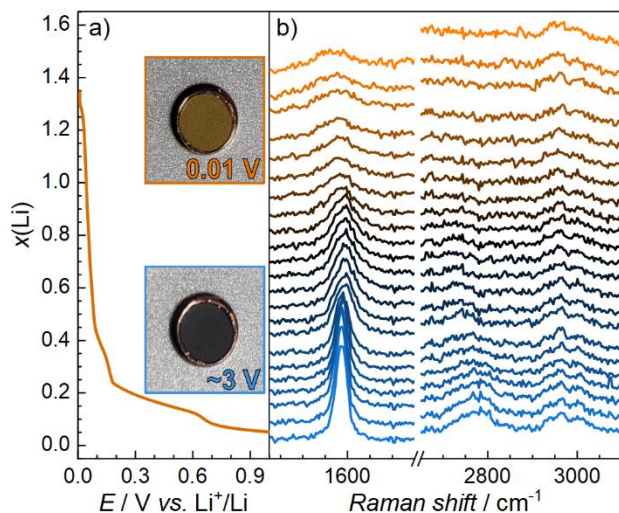


**Figure 2.** (a) Voltage profile of the graphite electrode and (b) the *operando* Kerr gated Raman spectra (stacked as a function of  $x(\text{Li})$ ) collected at 2 ps delay times showing the primary G and 2D graphite bands at 1580 and 2780  $\text{cm}^{-1}$ , respectively (electrolyte bands at *ca.* 2980  $\text{cm}^{-1}$ ). Inset images in a-i) show images of the electrode *via* the optical window before and after full lithiation to  $\text{LiC}_6$ .

Selected *operando*-collected Kerr gated Raman spectra are provided in Figure 2b stacked as a function of depth of lithiation (*i.e.*,  $x(\text{Li})$  in  $\text{LiC}_6$ ). Therein, the two key regions relating the G (1580  $\text{cm}^{-1}$ ) and 2D (2780  $\text{cm}^{-1}$ ) graphitic bands are presented. Additionally, bands relating to the C-H stretching modes of the electrolyte can also be observed at *ca.* 2980  $\text{cm}^{-1}$ . Upon discharging the half-cell (*i.e.*, intercalation of Li into the graphite working electrode), the G and 2D bands undergo changes as functions of the depth of lithiation, in agreement with previous reports.<sup>4,5,7</sup> Most importantly, in the early stages, the G band first undergoes a blue shift from 0.5 to 0.2 V *vs.*  $\text{Li}^+/\text{Li}$ . Subsequently, the G band undergoes a broadening and a continued red shift as the cell voltage proceeds below 0.2 V *vs.*  $\text{Li}^+/\text{Li}$ . This latter behaviour manifests as a peak splitting when probed by CW Raman microscopy, due to the differences in the interior  $\text{E}_{2g2}(\text{i})$  and bounding  $\text{E}_{2g2}(\text{b})$  modes.<sup>7</sup> However, the peak splitting is not observed in the Kerr gated Raman spectra which can be attributed to reduced spectral resolution and increased inhomogeneity of the measured area due to the Raster scanning nature of the Raman probe beam. Conversely, CW Raman microscopy measurements focus the probe beam onto individual graphite particles where the homogeneity would be expected to be more reliable. Critically however, after midway through the lithiation process, the Kerr gated Raman spectra still present clear G bands in all spectra including the fully intercalated  $\text{LiC}_6$  (*i.e.*, top spectra in Figure 2b). The Kerr gated Raman spectrum of the fully intercalated electrode is compared with the CW Raman spectrum and the equivalent ungated (400 nm) spectrum in Figure 3. Therein, only the Kerr gated Raman spectrum retains the spectral information that can be unambiguously assigned to the graphite G band. The loss of the G band from CW Raman spectra of highly lithiated graphite has previously been attributed to the overlap of growing fluorescence signals and the reduced optical skin depth of the more conductive lithiated state which reduces

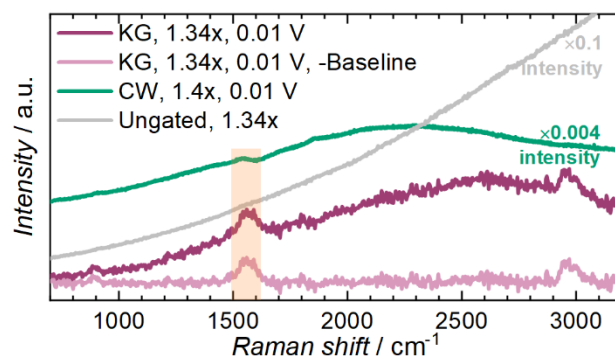


**Figure 3.** (a) Comparison of Kerr gated (KG) Raman spectra with conventional continuous wave (CW) Raman spectra and ungated spectra of fully lithiated  $\text{LiC}_6$ .

the scattering intensities. However, the efficacy of the Kerr gate in removing much of the background emission signals has enabled the retention of the graphite band even in the fully lithiated  $\text{LiC}_6$  electrode. We also demonstrated that these changes in the measured spectra are reversed upon charging of the half-cell (*i.e.*, deintercalation of the Li, not presented here).

## Conclusions

*Operando* electrochemical Kerr gated Raman spectroscopy was used to track the complete lithiation process of a graphite-based electrode. The effective fluorescence suppression achieved by employing the Kerr gate facilitated direct observation of the trends in the graphite G bands through the high states of charge from  $\text{Li}_{0.5}\text{C}_6$  through to  $\text{LiC}_6$ . These trends had been difficult to observe by conventional Raman spectroscopic methods. This could provide a powerful diagnostic tool to probe the higher states of charge in graphite negative electrodes in Li-ion cells.

## Acknowledgements

This work was supported by the UK Faraday Institution (EPSRC EP/S003053/1) through the Degradation Project (grant numbers FIRG001 and FIRG024).

## References

- Märker, K.; Xu, C.; Grey, C. P., *Operando* NMR of NMC811/Graphite Lithium-Ion Batteries: Structure, Dynamics, and Lithium Metal Deposition. *J. Am. Chem. Soc.* **2020**, *142*, 17447-17456, 10.1021/jacs.0c06727.
- Taminato, S.; Yonemura, M.; Shiotani, S.; Kamiyama, T.; Torii, S.; Nagao, M.; Ishikawa, Y.; Mori, K.; Fukunaga, T.; Onodera, Y.; Naka, T.; Morishima, M.; Ukyo, Y.; Adipranoto, D. S.; Arai, H.; Uchimoto, Y.; Ogumi, Z.; Suzuki, K.; Hirayama, M.; Kanno, R., Real-time observations of lithium battery reactions—*operando* neutron diffraction analysis during practical operation. *Sci. Rep.* **2016**, *6*, 28843, 10.1038/srep28843.
- Whitehead, A. H.; Edström, K.; Rao, N.; Owen, J. R., In situ X-ray diffraction studies of a graphite-based Li-ion battery negative electrode. *J. Power Sources* **1996**, *63*, 41-45, 10.1016/S0378-7753(96)02440-8.
- Inaba, M.; Yoshida, H.; Ogumi, Z.; Abe, T.; Mizutani, Y.; Asano, M., In Situ Raman Study on Electrochemical Li Intercalation into Graphite. *J. Electrochem. Soc.* **1995**, *142*, 20-26, 10.1149/1.2043869.
- Hardwick, L. J.; Buqa, H.; Novák, P., Graphite surface disorder detection using in situ Raman microscopy. *Solid State Ionics* **2006**, *177*, 2801-2806, 10.1016/j.ssi.2006.03.032.
- Cabo-Fernandez, L.; Neale, A. R.; Braga, F.; Sazanovich, I. V.; Kostecki, R.; Hardwick, L. J., Kerr gated Raman spectroscopy of  $\text{LiPF}_6$  salt and  $\text{LiPF}_6$ -based organic carbonate electrolyte for Li-ion batteries. *Phys. Chem. Chem. Phys.* **2019**, *21*, 23833-23842, 10.1039/C9CP02430A.
- Sole, C.; Drewett, N. E.; Hardwick, L. J., In situ Raman study of lithium-ion intercalation into microcrystalline graphite. *Faraday Discuss.* **2014**, *172*, 223-237, 10.1039/C4FD00079J.